

Article

Exergetic Analysis of DME Synthesis from CO₂ and Renewable Hydrogen

Marcello De Falco ^{1,*}, Gianluca Natrella ², Mauro Capocelli ¹, Paulina Popielak ³, Marcelina Sołtysik ³, Dariusz Wawrzynczak ³ and Izabela Majchrzak-Kucęba ³

¹ Unit of Process Engineering, Department of Engineering, Università Campus Bio-Medico di Roma, Via Álvaro del Portillo 21, 00128 Rome, Italy; m.capocelli@unicampus.it

² Dipartimento di Ingegneria Navale, Elettrica, Elettronica e delle Telecomunicazioni—DITEN, University of Genoa, DITEN, Via all'Opera Pia 11A, 16145 Genoa, Italy; gianluca.natrella@edu.unige.it

³ Department of Advanced Energy Technologies, Faculty of Infrastructure and Environment, Czestochowa University of Technology, Dabrowskiego 73, 42-201 Czestochowa, Poland; paulina.popielak@pcz.pl (P.P.); marcelina.soltysik@pcz.pl (M.S.); dariusz.wawrzynczak@pcz.pl (D.W.); izabela.majchrzak-kuceba@pcz.pl (I.M.-K.)

* Correspondence: m.defalco@unicampus.it; Tel.: +39-347-6809041



Citation: De Falco, M.; Natrella, G.; Capocelli, M.; Popielak, P.; Sołtysik, M.; Wawrzynczak, D.; Majchrzak-Kucęba, I. Exergetic Analysis of DME Synthesis from CO₂ and Renewable Hydrogen. *Energies* **2022**, *15*, 3516. <https://doi.org/10.3390/en15103516>

Academic Editors: Federica Raganati and Paola Ammendola

Received: 12 April 2022

Accepted: 9 May 2022

Published: 11 May 2022

Publisher's Note: MDPI stays neutral with regard to jurisdictional claims in published maps and institutional affiliations.



Copyright: © 2022 by the authors. Licensee MDPI, Basel, Switzerland. This article is an open access article distributed under the terms and conditions of the Creative Commons Attribution (CC BY) license (<https://creativecommons.org/licenses/by/4.0/>).

Abstract: Carbon Capture and Utilization (CCU) is a viable solution to valorise the CO₂ captured from industrial plants' flue gas, thus avoiding emitting it and synthesizing products with high added value. On the other hand, using CO₂ as a reactant in chemical processes is a challenging task, and a rigorous analysis of the performance is needed to evaluate the real impact of CCU technologies in terms of efficiency and environmental footprint. In this paper, the energetic performance of a DME and methanol synthesis process fed by 25% of the CO₂ captured from a natural gas combined cycle (NGCC) power plant and by the green hydrogen produced through an electrolyser was evaluated. The remaining 75% of the CO₂ was compressed and stored underground. The process was assessed by means of an exergetic analysis and compared to post-combustion Carbon Capture and Storage (CCS), where 100% of the CO₂ captured was stored underground. Through the exergy analysis, the quality degradation of energy was quantified, and the sources of irreversibility were detected. The carbon-emitting source was a 189 MW Brayton–Joule power plant, which was mainly responsible for exergy destruction. The CCU configuration showed a higher exergy efficiency than the CCS, but higher exergy destruction per non-emitted carbon dioxide. In the DME/methanol production plant, the main contribution to exergy destruction was given by the distillation column separating the reactor outlet stream and, in particular, the top-stage condenser was found to be the component with the highest irreversibility (45% of the total). Additionally, the methanol/DME synthesis reactor destroyed a significant amount of exergy (24%). Globally, DME/methanol synthesis from CO₂ and green hydrogen is feasible from an exergetic point of view, with 2.276 MJ of energy gained per 1 MJ of exergy destroyed.

Keywords: carbon capture and utilization; methanol and DME production; exergy analysis

1. Introduction

Climate change mitigation is a worldwide effort that involves all countries around the world. Among all problems, greenhouse gas (GHG) emissions have a significant impact on the environment. Regarding this matter, the Intergovernmental Panel on Climate Change (IPCC) and the United Nations Climate Change Conference have established the needs of reducing CO₂ emissions (recognized as the gas mainly responsible for climate change) and mitigating the global average temperature increase. Targets were set up, proposals to reach them were provided, and some technologies were identified as a solution in counteracting this issue.

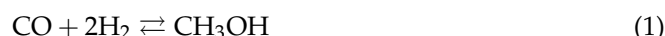
The extensive concentration of carbon dioxide in the atmosphere is a threat to environmental safety, contributing to the greenhouse effect, but CO₂ is a source of carbon for plants and can also be used as a reactant in chemical reactions [1–3]. This concept has led to the development of Carbon Capture and Utilization (CCU) technologies, which are perceived as a more justified and socially acceptable technology for CO₂ management than Carbon Capture and Storage (CCS). However, even if they can be considered a feasible solution, their cost is still an issue. Hasan et al. proposed a national Carbon Capture Utilization and Storage (CCUS) supply chain network for a U.S. case study in their multiscale framework analysis [4]. With the proposed solution focused on profit rather than maximizing CO₂ utilization, average profits between \$0.3 and \$17.6 per ton of CO₂ were achieved (depending on the weighted average total costs of capturing and utilizing a ton of CO₂).

There are plenty of ways to apply CCU technology wherever there is a CO₂-emitting source, e.g., energy-intensive industry branches, such as energy, petrochemical and cement or iron and steel production. Additionally, CCU reactions can be supported with green technologies, such as renewable energy sources (RES).

The first step in a CCU process is the capturing of CO₂ through well-known technologies, such as oxyfuel combustion, pre-combustion or post-combustion, or as a direct-air capture process [5,6]. Post-combustion carbon capture can be achieved by physical or chemical separation methods, such as membranes, adsorption, absorption and cryogenic processes. Many of these technologies are already applied in industry [7]. Pre-combustion processes capture CO₂ prior to the combustion reaction and it can be achieved with the coal gasification process or with oil or gas fuel-reforming processes [8].

After having captured and concentrated the CO₂, it can be fed to a chemical reactor for its conversion into products, such as syngas, urea, methane, ethanol, formic acid, etc. This paper is focused on the analysis of configurations to synthesize methanol and dimethyl ether (DME) from CO₂.

Dimethyl ether (DME) or methoxymethane is the simplest aliphatic ether with the molecular formula CH₃OCH₃. It is a colourless, near-odourless gas under ambient conditions. It is neither a toxic nor carcinogenic compound, with properties similar to liquid petroleum gas (LPG); thus, it can be easily blended with it and used as a fuel [9–11]. In the chemical industry, it is mainly used to produce diethyl sulphate, methyl acetate, light olefins and gasoline [12]. Nowadays, it is considered an alternative fuel with low emissions of NO_x, hydrocarbons and carbon monoxide [2,13]. DME can be obtained in two ways: direct synthesis and through the methanol dehydration process. The first method's reactions are:



The process of direct DME synthesis is exothermic (c.a. 246.2 kJ/mol DME); therefore, the heat produced during the reactions has to be removed. The inlet reactant mixture is composed of CO and H₂.

Methanol dehydration to produce DME is also an exothermic process. CO₂ can be used to produce methanol and then dehydrate it to DME. This has been proven to be a very economical way of utilizing carbon dioxide [2,14,15]. The chemical reactions occurring during the process are presented below:

Methanol formation



Methanol dehydration



Reverse water–gas shift (rWGS)



Net reaction



In Ref. [16], the authors explored the profitability of DME production from biogas; in Ref. [17], a techno-economic assessment of bio-DME and bio-methanol production from oil palm residue was proposed. Methanol is a colourless, flammable liquid under ambient conditions with a characteristic odour. As one of the most important raw materials, it is a substrate in many syntheses of chemical compounds, including formaldehyde, acetic acid and chloromethane. It is also a very good solvent and it is easily miscible with water, alcohols and organic solvents. Due to its wide application in many industries (fuel, chemical and other industries), the demand for methanol is constantly growing, i.e., from 47 Mt/a in 2011 [18] to 100 Mt/a in 2021 [19]. According to the report made by the International Renewable Energy Agency [19], in 2021, only 0.2% of global production of methanol came from renewable sources—more than 60% was converted by natural gas reformation and the rest was produced by natural coal gasification.

Methanol can be synthesized from a gas containing either carbon monoxide or carbon dioxide when it reacts with hydrogen:



The main properties of DME and methanol in comparison with LNG and diesel oil are shown in Table 1. Moreover, several potential major applications of DME and methanol are shown below in Figures 1 and 2.

Table 1. Properties of DME and methanol compared with other fuels.

Properties	DME [20]	Methanol [18]	Methane * [21]	Diesel Fuel [22,23]
Molecular formula	C ₂ H ₆ O	CH ₃ OH	CH ₄	—
CAS Number	115-10-6	67-58-1	74-82-8	68334-30-5
Molar mass (g/mol)	46.07	32.04	16.04	—
Cetane number **	55 to 60	~5	0	40 to 55
Melting point (°C)	−141	−97.88	−182.47	−40
Boiling point (°C) at 1 atm	−24.8	64.65	−161.5	141
Density at 25 °C and 1 atm (kg/m ³)	668.3	786.68	0.657	800–910
Autoignition temperature (°C)	235	440	537	250
Miscible with water?	Yes	Yes	Yes	No
Miscible with organic solvents? ***	Yes	Yes	Yes	Yes

* Methane as main part of Liquid Natural Gas (LNG), ** average value, *** with most popular polar and nonpolar organic solvents.

DIMETHYL ETHER

Fuel substitute

DME is considered to be a clean fuel of new generation, can be used as gasoline substitute or as jet fuel. Similar properties to LPG makes it possible to use/blend with it and applied to existing infrastructure.

Power generation

Primarily it can be successfully used as a fuel in gas turbines.

Diesel substitute

Diesel Oil engines can be easily modified to be able to burn DME as fuel (minor modification fuel injection system). Moreover DME offers greater efficiency of compression engines and lower emission of NOx and SOx in compare to diesel fuel.

Chemical production

Nowadays is mainly used as aerosol propellant in spray cans and substrate in olefins production.

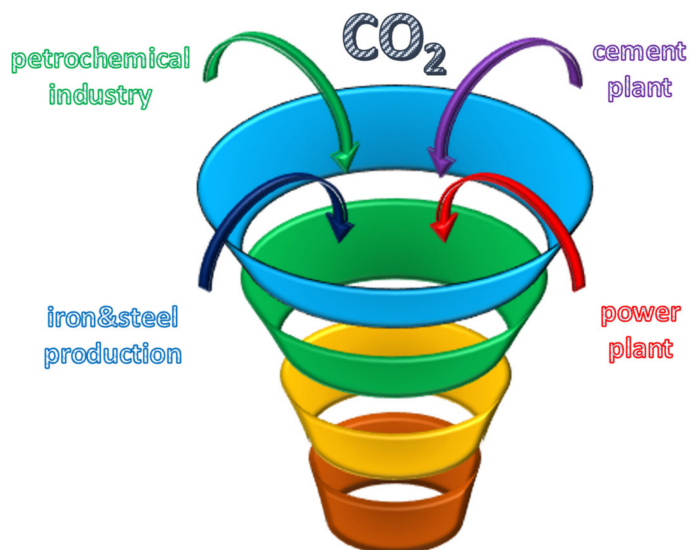
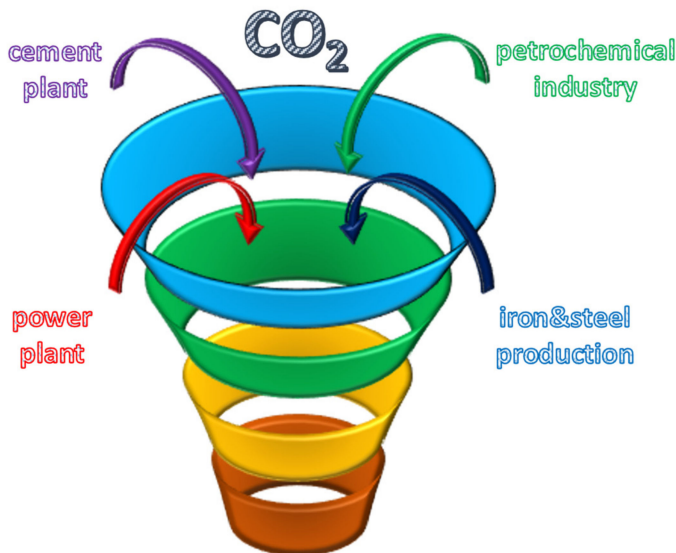


Figure 1. Applications of DME [20,24].

METHANOL



Fuel substitute

Methanol can be blended with gasoline in various ratio from 3% up to 10%. Additionally has high octane rating and high knocking resistance.

Power generation

Can be used in methanol-fired turbines, for cooking stoves, industrial boilers, furnaces and home heating.

Diesel substitute

Diesel Oil engines can be fuel by biodiesel which main component is methanol.

Chemical production

Methanol can be used as raw material for production of for example: formaldehyde, chloromethane and esters.

Figure 2. Applications of methanol [18,19,25].

State-of-the-Art Production of DME/Methanol from Green Hydrogen and CO₂

Converting CO₂ into DME requires an energy input in the form of hydrogen, as shown in Equations (1)–(9). In order to meet the goal of reducing carbon emissions, green hydrogen is needed [1,5,26,27].

Hydrogen can be synthesized in different ways: chemical, biological, catalytic, electrochemical and thermal. To reduce the carbon footprint of the CCU process, a low-emission hydrogen production technology has to be applied. Among several possible approaches, the production of “green hydrogen” using an electrolyser powered by a renewable energy source is the most interesting [28,29].

Barbato et al. [24] presented a process for carbon dioxide conversion to green methanol where CO₂ captured from a power plant was combined with hydrogen from an electrolyser

powered by hydropower energy. In the calculations and conclusions, the price (with cost calculations at the prevailing rate) of methanol production resulted to be 294 €/ton and it was successfully reduced by 20% compared to the price of methanol produced traditionally.

While there are a number of pilot or demonstration-scale facilities, there are a few commercial units producing either DME or methanol on an industrial scale. Regarding existing facilities with a power plant as a carbon dioxide source, two projects developed in Germany can be taken into consideration.

The first was funded by Europe's Horizon 2020 program (MefCO₂, Project No. 637016). Nine partners established in 2014 an international cooperation to research the feasibility of CCU technology along with the production of green methanol. The main aims of the project were to demonstrate the economic feasibility of utilizing captured CO₂ by converting it into a usable fuel, such as methanol, and further providing green hydrogen produced from excess energy from renewable sources. The source of carbon dioxide was a lignite-fired power plant located in Niederaussem, Germany. The project ended in 2019 with the development of one of the largest facilities in the European Union to synthesize methanol from CO₂ from flue gases, capable of producing 1 ton of methanol per day while capturing more than 1.5 tons of carbon dioxide per day [30–37].

Carbon Recycling International Ltd. (CRI, Reykjavik, Iceland), known for producing renewable methanol since 2007, participated in this project. CRI's pilot unit is located near Iceland's capital—Reykjavik. Industrial-scale green methanol production began in 2012 in the first pilot plant with an annual capacity of about 4000 tonnes of methanol (c.a. 12 t/d). The process is based on the conversion of CO₂ from geothermal sources with the hydrogen produced by water electrolysis using geothermal energy [1,36,38]. The methanol produced in this facility is used in a number of applications, including blending with gasoline, biodiesel production, and wastewater denitrification. Additionally, the CRI methanol production process reduces the environmental impact by 90% compared to conventional methods [19]. Furthermore, CRI, in cooperation with China Henan Shuncheng Group, developed in 2021 the world's first green methanol plant with a capacity of 110,000 tons per year [39].

The ALIGN-CCUS (Project No 271501) demonstration plant is also located at Niederaussem, Germany. The project was funded through the ERA-NET ACT program and it was co-funded by the European Commission under the Horizon 2020 program ACT [40]. The source of the captured CO₂ is a 1000 MW power plant unit, and the hydrogen comes from a 140 kWel alkaline electrolyser providing 22 kg of hydrogen per day. The daily production of DME is about 50 kg. For DME synthesis, a Mitsubishi Power bifunctional catalyst was used, which was responsible for both methanol synthesis and the dehydration process [41].

In this paper, we evaluate the energetic performance of a DME and methanol synthesis process fuelled by the CO₂ captured from a natural gas combined cycle (NGCC) power plant and by the green hydrogen produced using an electrolyser (alkaline). The process configuration performance is assessed by means of an exergetic analysis and compared to a post-combustion CCS. Through exergy, these two different processes can be evaluated [42–44], assessing the quality degradation of energy and individuating sources of irreversibility.

The post-combustion CCS is a common basis to compare new strategies to avoid carbon emissions. Olaleye et al. deeply discussed post-combustion carbon capture from a coal-fired power plant [45,46].

Blumberg et al. presented an NG-based low-pressure synthesis process for the production of methanol with CO₂ utilization [47]. In their paper, the authors conducted an extended exergy analysis dividing the methanol production plant into various subsystems and evaluated the performance of each of them. Nakayai et al. [48] conducted an energy and exergy analysis of the DME production from CO and CO₂ in a single-stage process. Farooqui et al. [49] evaluated from an energetic and an exergetic point of view a poly-generation plant with oxyfuel carbon capture for combined power and DME production. In our paper, we proposed a new configuration for DME and methanol production in a

single-stage process, in which a 90% CO₂ conversion rate was achieved. We compared this process with post-combustion CCS and evaluated all of the chain from the NGCC power plant to the DME and methanol production. Through the exergetic analysis, we spotted the irreversibilities, calculated the conventional performance indicators [45–47] and defined new performance indicators to assess the goodness of our configuration with respect to energy transformation and exergy destruction.

The proposed configuration is described in Section 2. Section 3 introduces the adopted methodology and the process assumptions that were made. Section 4 presents the results of the exergy analysis and Section 5 gathers the main conclusions of the work.

2. Systems Description

In this section, the proposed system to reduce carbon emissions and to produce valuable products, such as DME and methanol, is described (Figure 3). The carbon dioxide-emitting source is a natural gas combined cycle (NGCC) power plant whose flue gas is washed with an MDEA water solution to capture the CO₂ (refer to Section 2.1). The recovered carbon dioxide is partly stored underground and partly converted into DME and methanol, reported in Sections 2.2 and 2.3, respectively.

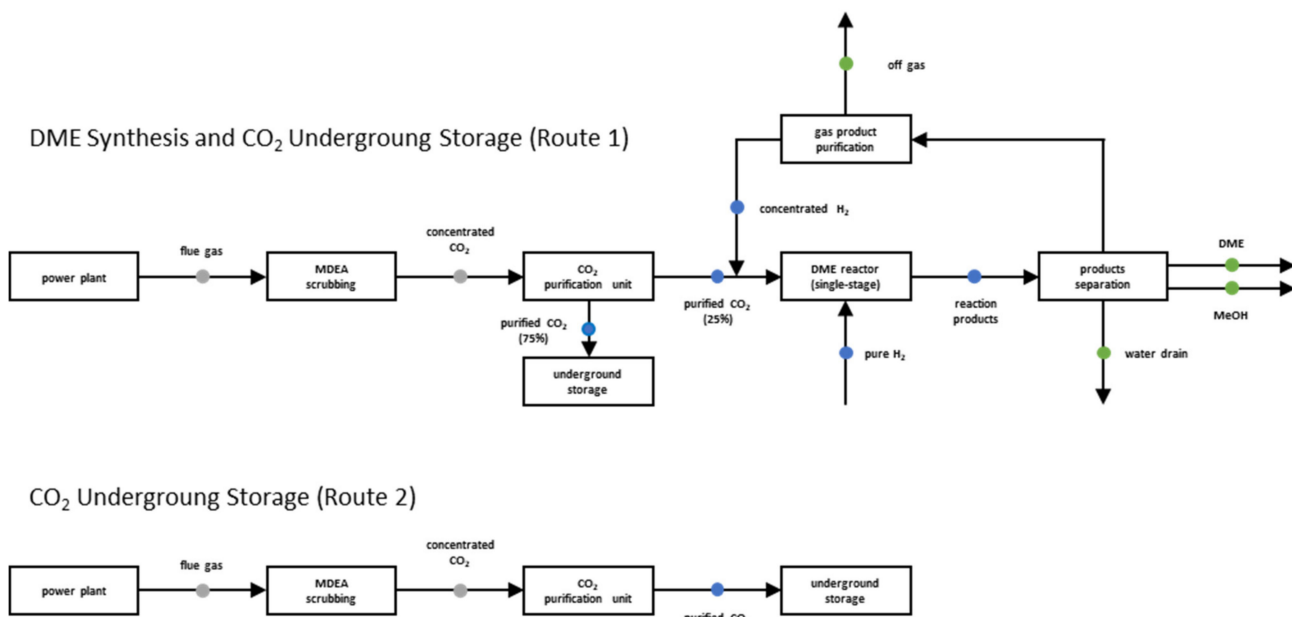


Figure 3. Configuration of the proposed solution (top) and of the comparison basis.

2.1. Power Plant and Post Combustion Carbon Capture

The simplified scheme of the NGCC power plant with Post-Combustion Carbon Capture (PCCC) is depicted in Figure 4. The parameters and process configuration are taken from [50]. The overall scheme is presented in Figure 4 and the main inputs, outputs and assumptions are listed in Table 2.

The Heat-Recovery Steam Generator (HRSG) of the power plant has three pressure levels:

- 4.6 bar, low pressure (LP);
- 40 bar, intermediate pressure (IP);
- 150 bar, high pressure (HP).

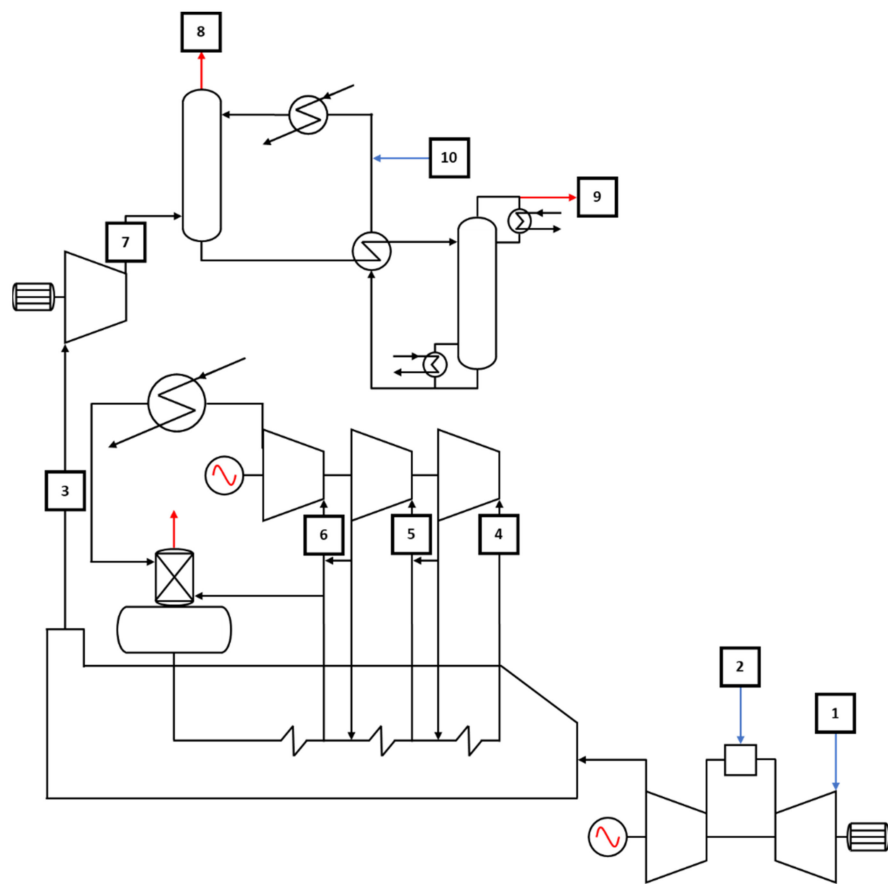


Figure 4. Power Plant—PCCC block scheme (the numbers represent the flow rates between the units).

Table 2. Power Plant and PCCC Process Assumptions.

Operating Parameter	Value
Natural Gas Flow Rate (kg/h)	50,000
Air Flow Rate (kg/h)	2,572,034
Compressed Air Pressure (bar)	18.2
Gas Turbine Outlet Temperature (K)	898
Compressors Polytropic Coefficients	0.9215–0.9315
Compressors Mechanical Efficiency	0.9
Turbines Mechanical Efficiency	0.9
TG Isentropic Efficiency	0.75
Water Flow Rate (kg/h)	169,197
High Pressure (bar)	150
Intermediate Pressure (bar)	40
Low Pressure (bar)	4.6
HT Isentropic Efficiency	0.92
IP Isentropic Efficiency	0.94
LP Isentropic Efficiency	0.88
Condensing Temperature (K)	311.5
Net Power from Power Plant (MW)	188.5
Solvent	40% MDEA (mass basis)
Absorber Pressure (bar)	3.8
Absorber Number of Stages	10
Stripper Pressure (bar)	1.1
Stripper Number of Stages	5
Stripper Reboiler	Kettle

The outlet steam of the low-pressure turbine (LT) is condensed and fed to the deaerator unit with the condensate pump (CP) at 3 bar. Here, a vent is purged and the liquid collected at the bottom is pressurized at 4.6 bar with the low-pressure pump (LPP) before being mixed with the almost-saturated liquid water from the reboiler of the stripper column in the PCCC unit. The resulting liquid stream is partially vaporized in the HRSG. The liquid and vapour are separated, the vapour fraction is further heated in the HRSG, the liquid fraction is once again split, one part is fed to the intermediate pressure pump (IPP) and the other part to the high-pressure pump (HPP). Both pressurized liquids are heated in the HRSG; a fraction of the IP liquid is used to preheat the natural gas entering the combustion chamber and recirculate it with the saturated water from the reboiler of the stripper. The HP superheated steam is expanded in the high-pressure turbine (HT) to 40 bar; it is then mixed with the IP superheated steam and reheated in the HRSG. The resulting IP superheated steam is expanded in the intermediate-pressure turbine (IT) to the LP level and again mixed with the LP superheated steam. The resulting stream is split to feed both the stripper reboiler and the deaerator. The remaining fraction is expanded in the LT.

The oxidant in the natural gas combustion is air, which is compressed at 18.2 bar in a three-stage intercooled compressor. After combustion, the flue gas is expanded in a turbine (GT) until 1.03 bar [50]. The gas leaves the GT and enters the HRSG at 898 K, where it is cooled to 437 K. The heat recovered in the HRSG supplies the Rankine cycle. In the HRSG, the flue gas is cooled to 303 K and subsequently compressed in a two-stage intercooled compressor at 4 bar to be fed to the PCCC unit. Condensed water is expelled at the outlet of each compression–refrigeration stage.

Flue gas is fed to an absorber working at 3.8 bar from the bottom of the column. In the outlet section, the CO₂-rich stream is sent to a stripper, where the weak bond between MDEA and CO₂ is thermally broken in the reboiler. The lean solvent is collected at the bottom of the stripper and recirculated to the absorber, while almost-pure CO₂ is collected at the top of the stripper.

In particular, the polytropic coefficient for compressors was set to equal 0.9215 for the inter-refrigerated stages and equal 0.9315 for the non-inter-refrigerated ones.

2.2. Underground Storage

One route to avoid carbon emissions is the underground storage of the captured CO₂. This is accomplished by purifying and pressurizing the CO₂ collected at the top of the stripper. Carbon dioxide can be stored at different thermodynamic conditions. In this work, we supposed storing it as a supercritical liquid. Therefore, the gas stream containing pure CO₂ was pressurized at 153 bar in a five-stage intercooled compressor. Carbon dioxide was liquefied and stored at 153 bar and 303 K. The overall scheme is presented in Figure 5 and the main inputs, outputs and assumptions are listed in Table 3.

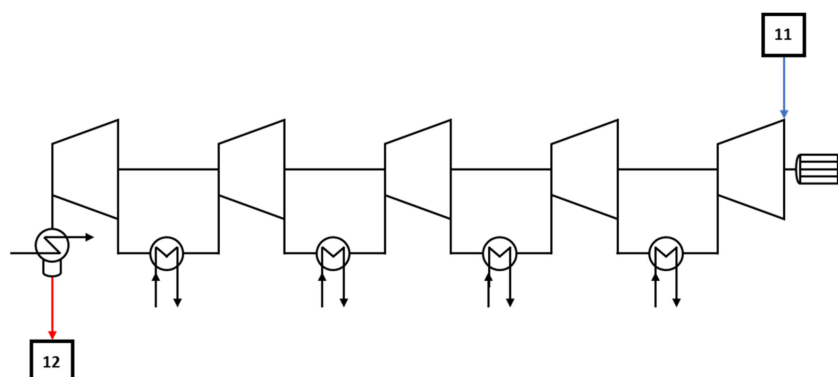


Figure 5. Underground storage block scheme (line 11 is the inlet pure CO₂ gas stream, line 12 is the pressurized and liquefied CO₂ stream).

Table 3. Underground storage process assumptions.

Operating Parameter	Value
Interstage Temperature (K)	303.15
Stored CO ₂ Temperature (K)	303.15
Stored CO ₂ Pressure (bar)	153
Pressure Drop at the inter coolers (bar)	0.2

2.3. DME Production Plant

As an alternative to total carbon dioxide geological storage, we considered carbon utilization for dimethyl ether (DME) production in a single-step reaction process. In this configuration, the DME production plant is fed with 25% of the total CO₂, leaving the remaining share destined to the underground storage as in the previously described case. Figure 6 shows the CO₂ conversion process scheme. A gaseous stream of CO₂ collected at the top of the stripper in the PCCC unit is purified and pressurized at 30 bar in a four-step intercooled compressor [51]. Then, the stream from the compressor is mixed with a pure H₂ stream and the stream recirculated from the top of the distillation column and containing CO₂ and H₂. The flow rate of H₂ has the value needed to achieve a hydrogen to carbon ratio (H/C) equal to 3. Then, the H₂-CO₂ mixture is heated up to 473.15 K and fed to the reactor, where the reactions of CO₂ hydrogenation, water–gas shift and methanol (MeOH) dehydration happen [51]:

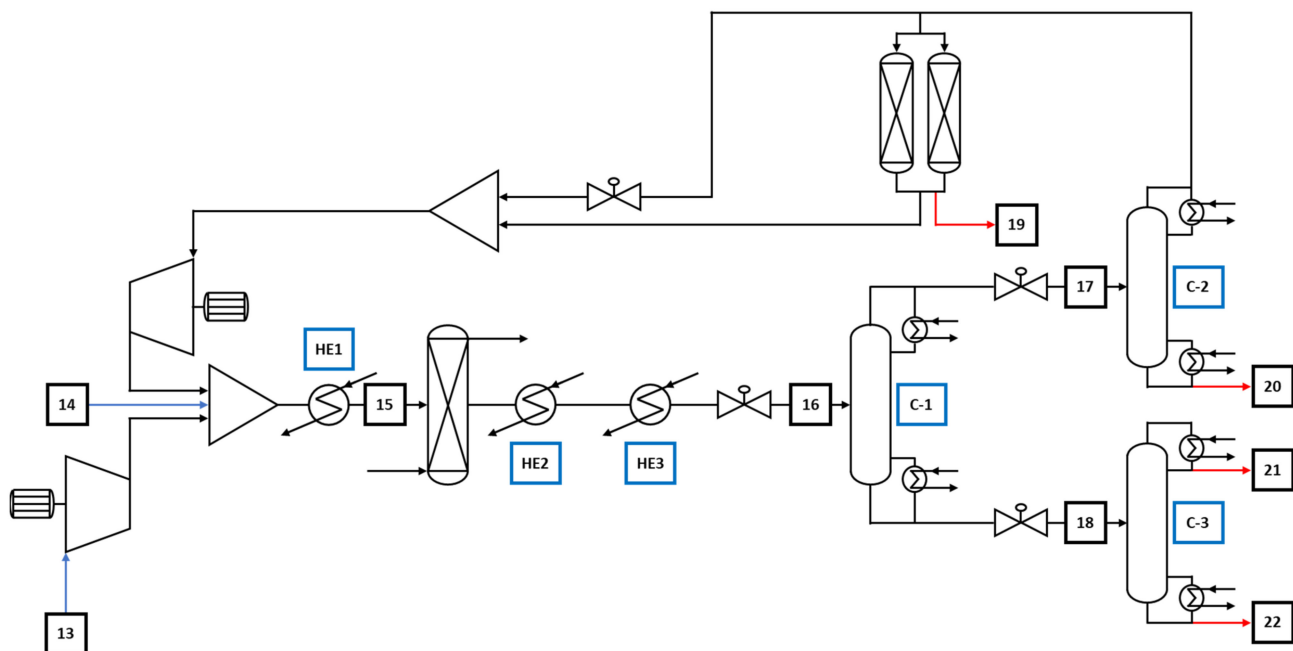


Figure 6. DME production plant block scheme (the tag HE represents the heat exchangers, the tag C represents the columns for product separation).

The heat generated by the exothermic reactions is removed from the reactor in order to maintain the temperature reaction constant at 473.15 K and supplied to the reboiler of column C-1. The duty from the reboiler covers around 43% of the thermal demand at the reboiler of column C-1. Then, the reaction products are cooled at 440 K in two heat

exchangers. The heat exchanger HE2 supplies the duty of the column C-3 reboiler, while the heat exchanger HE3 provides the heat needed by the column C-2 reboiler. After being cooled, the reaction products enter column C-1 at 21.3 bar. Here the heavy compounds, MeOH and water, are separated from the light ones (DME, CO, CO₂ and H₂). The light compounds are collected at the top of C-1 as a vaporous mixture and fed to column C-2 operating at 19 bar to separate the DME. The distillate of column C-2 contains unreacted CO, CO₂ and H₂, which are recycled to the reactor for 95% of their amount in the distillate, the remaining part enters a PSA to extract the hydrogen in it. Eighty percent of the hydrogen in the PSA is collected at the outlet section. The overall rate of CO₂ conversion is around 90%. MeOH and water are collected at the bottom of column C-1 as a liquid mixture and separated in column C-3 operating at 1.8 bar. Both columns C-1 and C-2 have partial condensers at their top stages working below the environmental temperature. In particular, the condensing temperatures at C-1 and C-2 are 262.48 K and 246.89 K, respectively. Therefore, refrigeration cycles are used to reach these temperatures, and 3.14 is the value supposed for the Coefficient of Performance (COP) of both cycles [52]. The overall scheme is presented in Figure 6 and the main inputs, outputs and assumptions are listed in Table 4.

Table 4. DME production plant process assumptions.

Operating Parameter	Value
Reactor Pressure (bar)	30
Reaction Temperature (K)	473.15
C-1 Pressure (bar)	20.5
C-1 Number of Stages	15
C-1 Condenser	Partial vapour
C-1 Reboiler	Kettle
C-2 Pressure (bar)	19
C-2 Number of Stages	15
C-2 Condenser	Partial vapour
C-2 Reboiler	Kettle
C-3 Pressure (bar)	1.8
C-3 Number of Stages	15
C-3 Condenser	Total
C-3 Reboiler	Kettle
COP	3.14

3. Assumptions and Methodology

All processes were simulated with the software Aspen Plus V10. The Peng–Robinson model was applied to the Brayton–Joule cycle of the power plant, while the Steam–Table model was chosen for the Rankine cycle of the plant. To control the process, eight design specifications were introduced to adjust the temperature at the outlet of the GT, the pinch temperature differences in the HRSG, the vent purge in the deaerator, the water make-up and the steam to be sent at the reboiler of the stripper in the PCCC unit. A calculator was used to evaluate the power generated by the plant. The natural gas properties were taken from [51]. The combustion chamber was simulated with an RGibbs reactor, which minimized the Gibbs free energy, and the deaerator with a Flash2 separator.

With respect to the PCCC unit, for all of the blocks within this unit, the ENRT-RK model was used, which consisted of an unsymmetric electrolyte NRTL model with the Redlich–Kwong equation of state and Henry's law for electrolyte systems. The electrolyte species were due to the presence of the amine MDEA as solvent.

To control the PCCC process, four design specifications were introduced to adjust the CO₂ content in the gas stream leaving the absorber from the top, the molar composition of the residue of the stripper, the water make-up and the solvent make-up. The absorber was simulated with a RadFrac column with no condenser nor reboiler of 10 theoretical stages working at 3.8 bar. The stripper was simulated with a RadFrac column too, without the

condenser, but with a Kettle reboiler fed with the LP steam from the power plant. It had five theoretical stages and a working pressure of 1.1 bar.

Regarding the DME production plant, the NRTL and the Peng–Robinson models were implemented. The former was for the distillation columns, which worked below 20 bar, and the latter was used for the other blocks, which worked at higher pressures. The single-stage reactor was modelled with an RGibbs reactor minimizing the Gibbs free energy with an implemented temperature approach of equilibrium of 20 K. The distillation columns used to separate the reaction products were all modelled with the RadFrac column. Every distillation column had 15 theoretical stages and a Kettle reboiler. Columns C-1 and C-2 were equipped with a partial condenser and their distillate was vaporous, while column C-3 had a total condenser providing a liquid distillate. DME was the primary product of the plant, while MeOH was a secondary product. The simulation included seven design specifications with the objective of setting the molar ratio between hydrogen and carbon at the inlet of the reactor and the distillates' flow rate and purity at each distillation column.

The exergy analysis with the aim of evaluating thermodynamics inefficiencies and rigorous performances of the process was based on the conventional methodology described in the following and found in some similar papers [45,47].

The ambient conditions were assumed at 298.15 K and 1.013 bar. The exergy flow rate E_i of the i -th stream was the sum of the physical and chemical exergies, as reported in Equation (13), and was obtainable from the Aspen Plus simulations, while the kinetic and potential exergies were neglected. For further details, please refer to [44].

$$E_i = E_i^{PH} + E_i^{CH} \quad (13)$$

The exergy destruction rate in the j -th component was calculated as follows:

$$E_{D,j} = E_{F,j} + E_{P,j} \quad (14)$$

where $E_{F,j}$, $E_{P,j}$ and $E_{D,j}$ are respectively the exergy of the streams fed to the j -th component, the exergy of the streams leaving the j -th component, and the exergy destroyed in the j -th component. Table 5 shows how $E_{F,j}$ and $E_{P,j}$ were defined for each component.

Table 5. Exergy of fuels and products for different components.

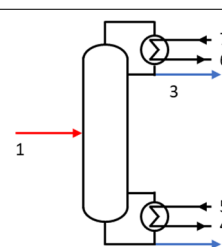
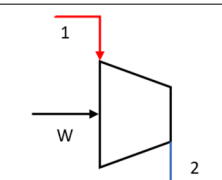
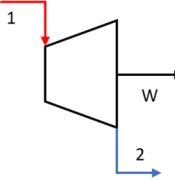
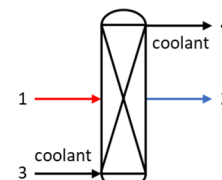
Component		E_F	E_P
Distillation Column		$E_5 - E_4$	$E_2 + E_3 - E_1 + E_6 - E_7$
Heat Exchanger		$E_3 - E_4$	$E_3 - E_1$
Compressor		$E_1 + W$	E_2

Table 5. Cont.

Component		E_F	E_P
Turbine		E_1	$E_2 + W$
Reactor		E_1	$E_2 - E_3 + E_4$
Valve		E_1	E_2

For every component, the following parameters were calculated:

$$\delta_j = \frac{E_{D,j}}{E_F} \quad (15)$$

$$\gamma_j = \frac{E_{D,j}}{\sum_j E_{D,j}} \quad (16)$$

where E_F is the sum of the exergy of the inlet streams in every process and E_P is the exergy of all the products of every process. For every unit, the exergy efficiency η is quantified by Equation (17).

The novel performance parameter ν is introduced for the PCCC, the underground storage and the DME production plant, defined by Equation (18) as the ratio between the destroyed exergy in the unit and the non-emitted CO_2 $m_{\text{CO}_2}^a$:

$$\eta = \frac{E_P}{E_F} \quad (17)$$

$$\nu = \frac{\sum_j E_{D,j}}{m_{\text{CO}_2}^a} \quad (18)$$

The values of the mass exergy of natural gas, DME, methanol and hydrogen were miscalculated by the software Aspen Plus V10; in fact, the software underestimated those values when the components were below their ignition point. The software mass exergy values for the streams carrying the above-mentioned components were corrected by adding the mass lower heating value weighted on the components' mass fraction in the stream. The standard lower heating value of natural gas was taken from [50]. The standard lower heating values of DME, methanol and hydrogen were taken from [53].

4. Results and Discussion

Exergy analysis was performed to detect the inefficiencies of the proposed process scheme, to locate the elements showing interesting improvement potentials and to compare the suggested hybrid solution (Route 1) to the complete underground storage (Route 2). The power plant and the PCCC were analysed with a process-integrated approach as they represented the common path for both process configurations. Instead, a very detailed exergy analysis on the underground storage unit and on the DME production plant was performed.

4.1. DME Synthesis and CO₂ Underground Storage Configuration (Route 1)

In this section, the exergy analysis of the proposed process solution to avoid carbon emissions is presented. The recovered carbon dioxide generated by the power plant was treated to be stored in geological sites for 75% and to be transformed into DME and MeOH for 25%. Table 6 shows the thermodynamic properties of the main material streams.

Table 6. Thermodynamic properties of selected material streams.

No.	Fluid	Unit	ξ (kJ/kg)	m (kg/h)	T (K)	P (bar)
1	Natural Gas	Power Plant	47,206	50,000	288.15	18.2
2	Air		0	2,572,034	298.15	1.013
3	Off Gas		1.877	2,622,034	303.15	1.03
4	H-Steam		1491	323,828	813.15	149.4
5	I-Steam		1390	378,823	813.50	39.2
6	L-Steam		719	168,047	489.37	3.4
7	Flue Gas	PCCC	122	2,532,475	303.15	3.8
8	Clean Gas		114	2,410,825	303.15	3.8
9	Captured CO ₂		5.13	125,015	294.11	1.1
10	Make up		1.36	3415	311.15	3.8
11	CO ₂	Underground Storage	4.75	89,288	294.11	1.1
12	Liquefied CO ₂		223	89,288	303.15	153
13	CO ₂	DME Production Plant	4.62	29,780	294.11	1.1
14	H ₂		120,000	3751.35	473.15	30
15	Reactants		15,991	108,554	473.15	30
16	C-1 Feed		15,586	108,554	440.63	21.3
17	C-2 Feed		17,858	89,061	262.48	19.5
18	C-3 Feed		4523.9	19,493	382.38	2.0
19	Off Gas		6580.8	3931	251.58	1.3
20	DME		26,662	10,444	343.10	19
21	MeOH		19,497	3293.3	349.60	1.8
22	Dirty Water		49.71	16,200	384.00	1.8

For every component j in the DME production plant, the exergy destruction $E_{D,j}$ and the parameters δ_j and γ_j were calculated based on the method reported in Table 5.

The exergetic efficiencies of the different units were calculated as follows:

$$\eta_{BJ} = \frac{W_{NET,BJ} + E_{HRSG}}{E_2} \quad (19)$$

$$\eta_R = \frac{W_{NET,R} + E_{Reb}}{E_{HRSG}} \quad (20)$$

$$\eta_{PCCC} = \frac{E_8 + E_9}{E_{reb} + W_{PCCC} + E_3} \quad (21)$$

$$\eta_{US} = \frac{E_{12}}{E_{11} + W_{US}} \quad (22)$$

$$\eta_{DME} = \frac{E_{19} + E_{20} + E_{21} + E_{22}}{E_{13} + E_{14} + W_{DME} + E_{F,HE1} + E_{F,C-3}} \quad (23)$$

where $W_{NET,BJ}$ and $W_{NET,R}$ are the net electric power in the Brayton–Joule and Rankine cycles, E_{HRSG} is the exergy exchanged in the Heat Recovery Steam Generator, E_i is the exergy associated with the i -th stream in Figure 4, E_{Reb} is the exergy exported to the reboiler of the stripper in the PCCC unit, and W_{PCCC} and W_{DME} are the electric power demand in the PCCC and DME production plant units, respectively. The exergy associated with the compressor of the off gas (stream no. 3 in Figure 4) was counted in the PCCC unit. The heat exchanger HE1 in Figure 6 heated up the reactants to 473.15 K; such an amount of heat was not recovered from anywhere in the process and it was supposed to be provided by a hot source at a constant temperature of 488.15 K. Instead, HE2 and HE3 supplied the heat

at the reboilers of C-3 and C-2 respectively. Approximately 42.65% of the heat needed at the reboiler of C-3 was supplied by the exothermic reactions (1)–(3). The remaining part was supposed to be provided by a hot source at a constant temperature of 479.64 K (15 K higher than the temperature at the reboiler of C-3). Therefore, the values of $E_{F,HE1}$ and of $E_{F,C-3}$ were calculated as shown in [54].

The values of η_{BJ} , η_R , η_{PCC} , η_{US} and η_{DME} , as well as the values of the destroyed exergies in the unit, are listed in Table 7, where the results of the exergy analysis of the different units are listed. The destroyed exergy in each unit was given by the difference between the denominator and the nominator of the corresponding exergy efficiency.

Table 7. Exergy analysis results.

Unit	E_D (MW)	η (%)	v (MJ/kg)
Brayton-Joule Cycle	277.90	45.57	
Rankine Cycle	108.96	50.05	
PCCC	150.23	36.96	40.80
Underground Storage	3.25	62.96	0.13
DME Production Plant	41.09	75.74	4.97

Figures 7 and 8 show the result of the exergy analysis of the DME production plant. The distillation column C-1 was mainly responsible for the exergy destruction, as it represented 45.19% of all exergy destruction, and its impact on exergy fuel reduction was worth 12.37%. In particular, the refrigeration cycle at the top stage of C-1 was the operation associated with the highest irreversibility, as shown in Figure 9. These values were higher than those of columns C-2 and C-3, because column C-1 dealt with higher flow rates and separated very different chemical species. Furthermore, as shown in Table 6, much of the stream fed to column C-1 left the column from the top at a temperature lower than the feed temperature. This fact determines the high exergy destruction in the column C-1 condenser. The reactor was the second-most responsible unit for exergy destruction, and column C-3 was the third. In particular, the exergy destruction associated with column C-3 was due to the difference in the specific exergy ξ of the streams. This is shown in Table 6; in fact, the specific exergy of the residue ξ_{22} was lower than the specific exergy of the feed ξ_{18} and specifically of the distillate ξ_{21} , but the mass flow of the residue was almost five times the mass flow of the distillate. The exergy destruction associated with the reactor was also due to the chemical exergy difference in reagents and products.

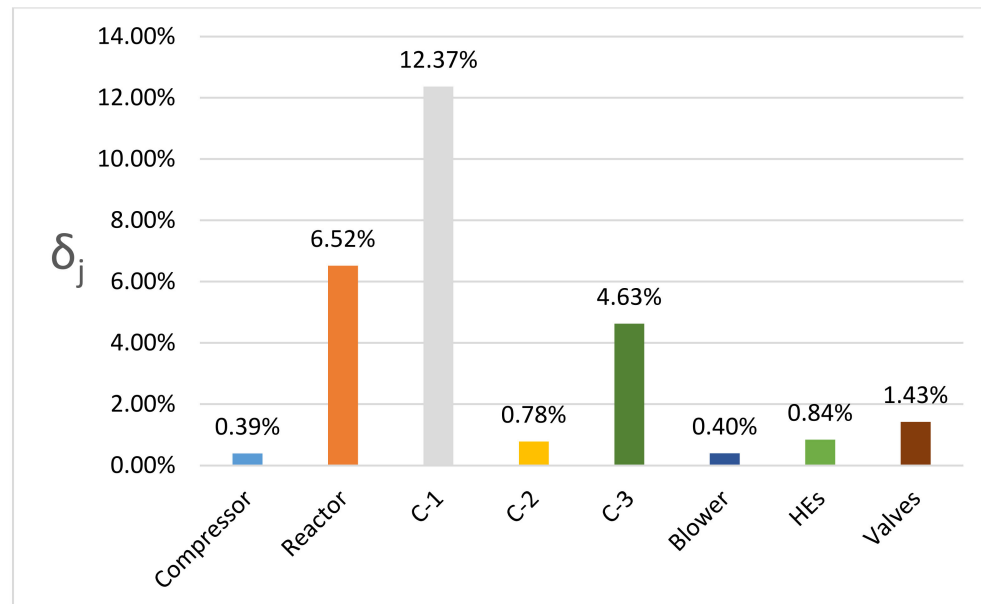


Figure 7. Percentage of fuel exergy ($E_F = 150.13$ MW) destroyed per component.

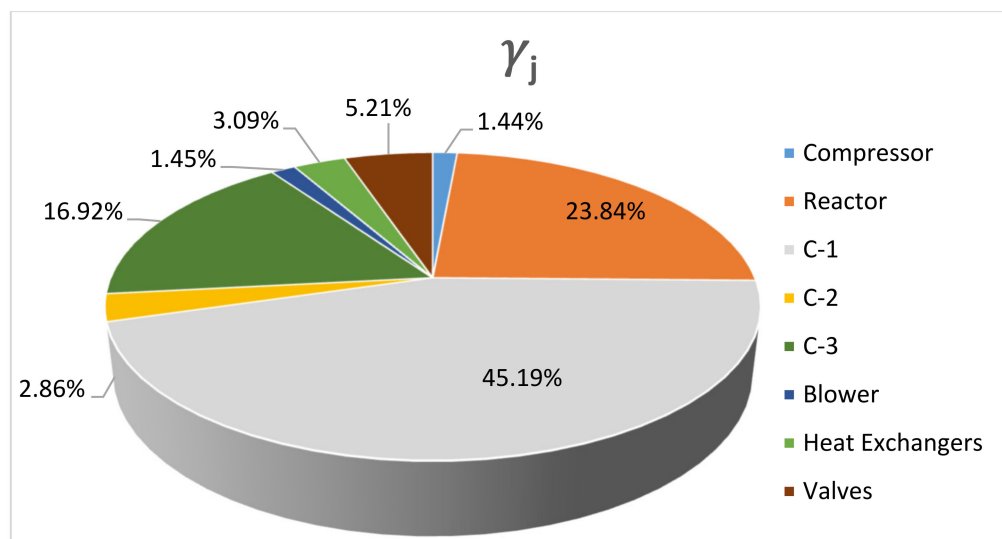


Figure 8. Percentage of destroyed exergy per component ($\sum_j E_{D,j} = 41.09 \text{ MW}$).

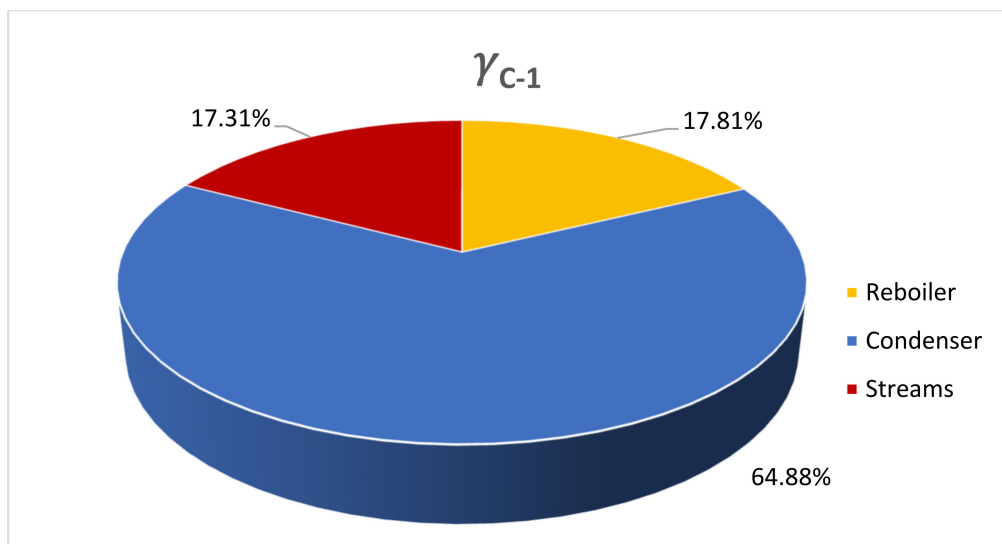


Figure 9. Distribution of destroyed exergy in C-1.

Figure 10 shows how the exergy destructions were distributed among the units. The Brayton–Joule cycle was mainly responsible for exergy destruction [55], while underground storage had the lowest impact.

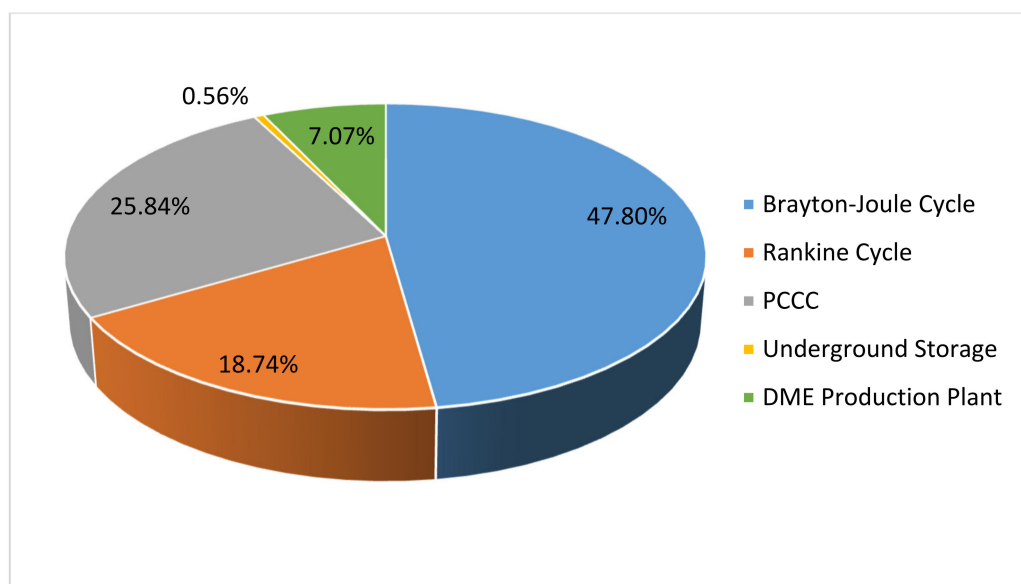


Figure 10. Distribution of exergy destruction between the units (total $E_D = 581.43$ MW).

4.2. Comparison with CO₂ Underground Storage (Route 2)

The results of the previous section are hereby compared with the Route 2 solution to avoid carbon emissions, i.e., 100% underground storage of recovered CO₂. The same power plant and PCCC were analysed; therefore the results for those units were the same as those in Route 1. The recovered carbon dioxide was supposed to be treated in order to be completely stored in geological sites. The thermodynamic properties of the material streams of the power plant and PCCC units in Table 6 are still valid. Figure 11 shows the exergy destruction distribution among the units.

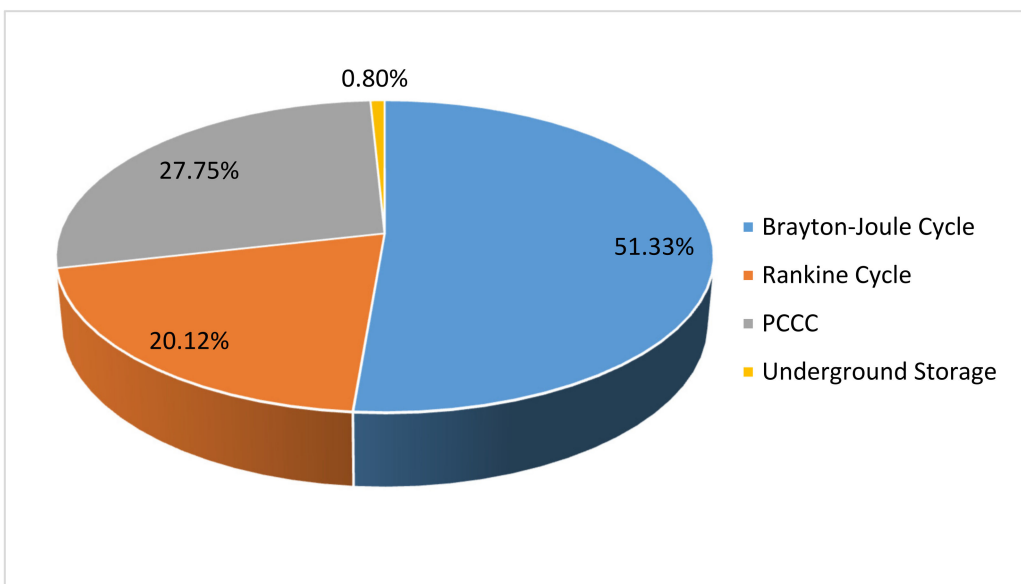


Figure 11. Distribution of exergy destruction between the units (total $E_D = 541.42$ MW).

The same conditions for temperature and pressure were set for the underground stored carbon dioxide in both routes, as shown in Tables 6 and 8. Therefore, the exergy efficiencies of the underground storage unit in Route 1 and in Route 2 were the same, but exergy destruction in this case accounted for 4.33 MW.

Table 8. Thermodynamic properties of selected stream materials.

No.	Fluid	Unit	ξ (kJ/kg)	m (kg/h)	T (K)	P (bar)
11	CO ₂	Underground Storage	4.75	119,068	294.11	1.1
12	Liquefied CO ₂		223	119,068	303.15	153

The results show a decrease in the total exergy destruction of 6.88% due to the complete storage of the recovered carbon dioxide. Focusing on the units treating the recovered CO₂, the destroyed exergy in Route 2 was approximately a tenth of the destroyed exergy in Route 1 (44.34 MW). Despite the consistent reduction in the destroyed exergy, the DME production plant unit had higher exergy efficiency than the underground storage unit. The process' intrinsic exergy efficiency was higher, but the additional use of high-value energy and material streams increased the overall exergy destruction. The exergy efficiencies and the destroyed exergy per non-emitted CO₂ coefficient are presented in Table 9 for the units treating the recovered CO₂.

Table 9. Comparison between the Route 1 and Route 2 CO₂-treating units.

	η (%)	v (MJ/kg)	Avoided CO ₂
Route 1	75.03	1.34	97.50%
Route 2	62.96	0.13	100%

Furthermore, the DME production plant unit was able to release available energy to the environment in the form of DME and MeOH streams. This energy value was quantified with the lower heating value of material streams 20 and 21 in Figure 6. The energy gain (EG) we obtained from DME and MeOH production in the DME production plant was calculated as the ratio between the sum of the energy transported by streams 20 and 21 and the exergy destroyed in the Route 1 CO₂-treating units:

$$EG = \frac{m_{20}LHV_{20} + m_{21}LHV_{21}}{E_{D,US} + E_{D,DME}} \quad (24)$$

The EG value is 2.276 MJ/MJ; in particular, it was 1.875 MJ/MJ for DME production and 0.401 MJ/MJ for MeOH production.

5. Conclusions

In the present study, an exergy analysis of a process configuration able to avoid carbon emissions and to produce DME and methanol is presented. The carbon-emitting source in this study was a 189 MW power plant. The Brayton–Joule cycle in the power plant was mainly responsible for exergy destruction, 75% of the produced carbon dioxide was captured to be stored underground and the remaining 25% was to be transformed into DME and methanol via reactions with hydrogen. In the plant, the total CO₂ generated by the power cycle was 119,068 kg/h, the amount stored was 89,288 kg/h, the stream converted was 26,815 kg/h and the amount vented to the atmosphere was 2965 kg/h (2.5% of the total). The reaction sections converted the CO₂ stream into DME (10,381 kg/h) and methanol (3214.1 kg/h). A second route was considered, i.e., the storage of 100% of the CO₂ generated by the power plant.

Of those two routes to avoid carbon emissions, the underground storage offers a much lower exergy destruction per mass of non-emitted carbon. Inside the DME production plant, the main contribution to exergy destruction was from the distillation column separating the reactor outlet stream and, in particular, the top-stage condenser was found to be the component with the highest irreversibility. This DME synthesis showed a higher efficiency than the underground storage unit, but a higher exergy destruction per non-emitted carbon dioxide ratio. As a consequence, the process configuration we propose has higher energetic efficiency and exergy destruction than full geological storage, and produces valuable compounds, such as DME and methanol. Its feasibility is strictly correlated with the

development of the hydrogen industry, and a future study should evaluate the impact of hydrogen production at different carbon dioxide shares between DME production and underground storage. Future works should investigate the optimal CO₂ split between Route 1 and Route 2 and extend exergy analysis to green hydrogen production.

Author Contributions: Conceptualization, M.D.F., D.W., G.N. and M.C.; methodology, G.N., M.C. and M.D.F.; software, G.N.; validation, M.D.F., D.W. and G.N.; formal analysis, G.N., M.C. and M.D.F.; investigation, G.N., M.C. and M.D.F.; resources, P.P., M.S. and G.N.; data curation, G.N., M.D.F. and D.W.; writing—original draft preparation, G.N. and M.D.F.; writing—review and editing, P.P., D.W., I.M.-K., M.S. and M.D.F.; visualization, G.N. and P.P.; supervision, M.D.F., D.W. and I.M.-K.; project administration, M.D.F., D.W. and I.M.-K.; funding acquisition, M.D.F., D.W. and I.M.-K. All authors have read and agreed to the published version of the manuscript.

Funding: This article has been supported by the Polish National Agency for Academic Exchange under Grant No. PPI/APM/2019/1/00042/U/00001.

Conflicts of Interest: The authors declare no conflict of interest.

Nomenclature

DME	Dimethyl Ethanol
MeOH	Methanol
NGCC	Natural Gas Combined Cycle
PCCC	Post-Combustion Carbon Capture
HRSG	Heat Recovery Steam Generator
HP	High-Pressure Level
IP	Intermediate-Pressure Level
LP	Low-Pressure Level
GT	Gas Turbine
HT	High-Pressure Turbine
IT	Intermediate-Pressure Turbine
LT	Low-Pressure Turbine
C-x	Distillation Column number x
HEx	Heat Exchanger number x
H/C	Hydrogen to Carbon ratio
COP	Coefficient of Performance
EG	Energy Gain
E_i	Exergy flow rate of <i>i</i> -th material stream
E_i^{PH}	Physical Exergy flow rate of <i>i</i> -th material stream
E_i^{CH}	Chemical Exergy flow rate of <i>i</i> -th material stream
$E_{D,j}$	Desstroyed Exergy flow rate in the <i>j</i> -th component
$E_{F,j}$	Fuel Exergy flow rate to the <i>j</i> -th component
$E_{P,j}$	Product Exergy flow rate of the <i>j</i> -th component
ξ	Specific Mass Exergy
m	Mass flow rate
$m_{CO_2}^a$	Mass flow rate of avoided CO ₂
δ_j	Destroyed Exergy to Fuel Exergy ratio for the <i>j</i> -th component
γ_j	Specific Destroyed Exergy in the <i>j</i> -th component
v	Destroyed exergy per avoided carbon emissions
η	Exergetic Efficiency
T	Temperature
P	Pressure

References

1. Majchrzak-Kucęba, I.; Szymanek, P. CCU Technologies in the Green Economy. *Eng. Prot. Environ.* **2018**, *21*, 261–271. [CrossRef]
2. Catizzone, E.; Bonura, G.; Migliori, M.; Frusteri, F.; Giordano, G. CO₂ recycling to dimethyl ether: State-of-the-art and perspectives. *Molecules* **2018**, *23*, 31. [CrossRef] [PubMed]
3. Masson-Delmotte, V.P.; Zhai, A.; Pirani, S.L.; Connors, C.; Péan, S.; Berger, N.; Caud, Y.; Chen, L.; Goldfarb, M.I.; Gomis, M.; et al. *The Physical Science Basis. Contribution of Working Group I to the 552 Sixth Assessment Report of the Intergovernmental Panel on Climate Change*; Cambridge University Press: Cambridge, UK; New York, NY, USA, 2021.
4. Hasan, M.M.F.; First, E.L.; Boukouvala, F.; Floudas, C.A. A multi-scale framework for CO₂ capture, utilization, and sequestration: CCUS and CCU. *Comput. Chem. Eng.* **2015**, *81*, 2–21. [CrossRef]
5. Koytsoumpa, E.I.; Bergins, C.; Kakaras, E. The CO₂ economy: Review of CO₂ capture and reuse technologies. *J. Supercrit. Fluids* **2018**, *132*, 3–16. [CrossRef]
6. Leung, D.Y.C.; Caramanna, G.; Maroto-Valer, M.M. An overview of current status of carbon dioxide capture and storage technologies. *Renew. Sustain. Energy Rev.* **2014**, *39*, 426–443. [CrossRef]
7. Chauvy, R.; De Weireld, G. CO₂ Utilization Technologies in Europe: A Short Review. *Energy Technol.* **2020**, *8*, 2000627. [CrossRef]
8. Dieterich, V.; Buttler, A.; Hanel, A.; Spliethoff, H.; Fendt, S. Power-to-liquid via synthesis of methanol, DME or Fischer-Tropsch-fuels: A review. *Energy Environ. Sci.* **2020**, *13*, 3207–3252. [CrossRef]
9. Lee, D.; Lee, J.S.; Kim, H.Y.; Chun, C.K.; James, S.C.; Yoon, S.S. Experimental study on the combustion and no x emission characteristics of DME/LPG blended fuel using counterflow burner. *Combust. Sci. Technol.* **2012**, *184*, 97–113. [CrossRef]
10. Kim, H.J.; Suh, H.K.; Park, S.H.; Lee, C.S. An experimental and numerical investigation of atomization characteristics of biodiesel, dimethyl ether, and biodiesel-ethanol blended fuel. *Energy Fuels* **2008**, *22*, 2091–2098. [CrossRef]
11. Wang, S.; Fu, Z. Thermodynamic and economic analysis of solar assisted CCHP-ORC system with DME as fuel. *Energy Convers. Manag.* **2019**, *186*, 535–545. [CrossRef]
12. Cheng, C.; Zhang, H.; Ying, W.; Fang, D. Intrinsic kinetics of one-step dimethyl ether synthesis from hydrogen-rich synthesis gas over bi-functional catalyst. *Korean J. Chem. Eng.* **2011**, *28*, 1511–1517. [CrossRef]
13. Zhang, Y.; Zhang, S.; Benson, T. A conceptual design by integrating dimethyl ether (DME) production with tri-reforming process for CO₂ emission reduction. *Fuel Process. Technol.* **2015**, *131*, 7–13. [CrossRef]
14. Catizzone, E.; Freda, C.; Bracco, G.; Frusteri, F.; Bonura, G. Dimethyl ether as circular hydrogen carrier: Catalytic aspects of hydrogenation/dehydrogenation steps. *J. Energy Chem.* **2021**, *58*, 55–77. [CrossRef]
15. Bonura, G.; Todaro, S.; Frusteri, L.; Majchrzak-Kucęba, I.; Wawrzyniczak, D.; Pászti, Z.; Tálas, E.; Tompos, A.; Ferenc, L.; Solt, H.; et al. Inside the reaction mechanism of direct CO₂ conversion to DME over zeolite-based hybrid catalysts. *Appl. Catal. B Environ.* **2021**, *294*, 120255. [CrossRef]
16. Baena-Moreno, F.M.; Gonzalez-Castaño, M.; Arellano-García, H.; Reina, T.R. Exploring profitability of bioeconomy paths: Dimethyl ether from biogas as case study. *Energy* **2021**, *225*, 120230. [CrossRef]
17. Im-orb, K.; Arpornwichanop, A. Comparative techno-economic assessment of bio-methanol and bio-DME production from oil palm residue. *Energy Convers. Manag.* **2022**, *258*, 115511. [CrossRef]
18. Ott, J.; Gronemann, V.; Pontzen, F.; Fiedler, E.; Grossmann, G.; Kersebohm, B.; Weiss, G.; Witte, C. Methanol. In *Ullmann's Encyclopedia of Industrial Chemistry*; Wiley-VCH Verlag GmbH & Co.: Berlin, Germany, 2012.
19. Kang, S.; Boshell, F.; Goeppert, A.; Prakash, S.G.; Landälv, I. *Innovation Outlook: Renewable Methanol*; IRENA: Abu Dhabi, United Arab Emirates, 2021.
20. Müller, M.; Hübsch, U. Dimethyl Ether. In *Ullmann's Encyclopedia of Industrial Chemistry*; Wiley-VCH Verlag GmbH & Co.: Berlin, Germany, 2000.
21. PubChem. Available online: <https://pubchem.ncbi.nlm.nih.gov/compound/Methane> (accessed on 17 February 2022).
22. Trafigura. Available online: https://www.trafigura.com/media/1687/en_sds_fuel-diesel-vgo_cas-68334-30-5.pdf (accessed on 17 February 2021).
23. Speight, J.G. *Handbook of Petroleum Product Analysis*; Wiley: Hoboken, NJ, USA, 2015; Volume 53.
24. Barbato, L.; Iaquaniello, G.; Mangiapane, A. Reuse of CO₂ to Make Methanol Using Renewable Hydrogen. In *CO₂: A Valuable Source of Carbon*; De Falco, M., Iaquaniello, G., Centi, G., Eds.; Green Energy and Technology; Springer: London, UK, 2013. [CrossRef]
25. Hobson, C.; Marquez, C. *Renewable Methanol Report*; Methanol Institute: Brussels, Belgium, 2018.
26. Huang, C.H.; Tan, C.S. A Review: CO₂ Utilization. *Aerosol Air Qual. Res.* **2014**, *14*, 480–499. [CrossRef]
27. de Falco, M.; Iaquaniello, G.; Centi, G. *CO₂: A Valuable Source of Carbon*; Green Energy and Technology; Springer: London, UK, 2013; Volume 137. [CrossRef]
28. Scott, K. *Sustainable and Green Electrochemical Science and Technology*; John Wiley and Sons Ltd.: Hoboken, NJ, USA, 2016.
29. Pérez-Fortes, M.; Schöneberger, J.C.; Boulamanti, A.; Tzimas, E. Methanol synthesis using captured CO₂ as raw material: Techno-economic and environmental assessment. *Appl. Energy* **2016**, *161*, 718–732. [CrossRef]
30. RWE. Available online: <https://www.rwe.com/en/press/rwe-power/2019-05-28-niederaussem-becomes-the-setting-for-important-technological-progress> (accessed on 22 February 2022).
31. MefCO₂. Available online: <http://www.mefCO2.eu/> (accessed on 21 February 2022).

32. Freyr, Ó.; Magistri, L.; Licozar, B.; Diaz, A.S. Green Methanol for a Green Future. MefCO₂. 2020. Available online: <http://www.mefco2.eu/news/green-methanol-for-a-green-future.php> (accessed on 23 February 2022).
33. Fernández-González, J.; Rumayor, M.; Domínguez-Ramos, A.; Irabien, A. Hydrogen Utilization in the Sustainable Manufacture of CO₂-Based Methanol. *Ind. Eng. Chem. Res.* **2022**. [CrossRef]
34. European Commission. Available online: <https://cordis.europa.eu/article/id/257671-energyintensive-sectors-can-be-part-of-low-carbon-transition> (accessed on 21 February 2022).
35. Ayala, P. Methanol Fuel from CO₂. Synthesis of Methanol from Captured Carbon Dioxide Using Surplus Electricity. MefCO₂. 13 September 2018. Available online: <https://etipwind.eu/wp-content/uploads/MefCO2-slides.pdf> (accessed on 23 February 2022).
36. Danish Energy Agency Technology Data for Renewable Fuels. 2017. Available online: <https://ens.dk/en/our-services/projections-and-models/technology-data/technology-data-renewable-fuels> (accessed on 24 February 2022).
37. Harp, G.; Tran, K.C.; Bergins, C.; Buddenberg, T.; Drach, I.; Sigurbjornsson, O. Application of Power to Methanol Technology to Integrated Steelworks for Profitability, Conversion Efficiency, and CO₂ Reduction. In Proceedings of the METEC 2nd ESTAD, Düsseldorf, Germany, 15–19 June 2016.
38. Andrei, B.D.; del Mar, P.F.M.; Evangelos, T.; Thea, S. *Carbon Capture and Utilisation Workshop: Background and Proceedings*; Publications Office of the European Union: Luxembourg, 2013.
39. Carbon Recycling International Ltd. Available online: <https://www.carbonrecycling.is/> (accessed on 22 February 2022).
40. Mann, I. Deep Decarbonisation is Within Reach of Europe’s Industrial Regions. March 2021. Available online: <https://www.alignccus.eu/news/align-ccus-findings-unveiled-deep-decarbonisation-within-reach-europe%E2%80%99s-industrial-regions> (accessed on 24 February 2022).
41. van Os, P. Accelerating low carbon industrial growth through carbon capture, utilization and storage (CCUS). *Greenh. Gases Sci. Technol.* **2018**, *8*, 994–997. [CrossRef]
42. Moran, M.J.; Sciuibba, E. Exergy Analysis: Principles and Practice. *J. Eng. Gas Turbines Power* **1994**, *116*, 285–290. [CrossRef]
43. Mistry, K.H.; Lienhard, J.H. Generalized least energy of separation for desalination and other chemical separation processes. *Entropy* **2013**, *15*, 2046. [CrossRef]
44. Bejan, A. *Advanced Engineering Thermodynamics*; John Wiley & Sons: Hoboken, NJ, USA, 2016.
45. Olaleye, A.K.; Wang, M.; Kelsall, G. Steady state simulation and exergy analysis of supercritical coal-fired power plant with CO₂ capture. *Fuel* **2015**, *151*, 57–72. [CrossRef]
46. Olaleye, A.K.; Wang, M. Conventional and advanced exergy analysis of post-combustion CO₂ capture based on chemical absorption integrated with supercritical coal-fired power plant. *Int. J. Greenh. Gas Control* **2017**, *64*, 246–256. [CrossRef]
47. Blumberg, T.; Morosuk, T.; Tsatsaronis, G. Exergy-based evaluation of methanol production from natural gas with CO₂ utilization. *Energy* **2017**, *141*, 2528–2539. [CrossRef]
48. Nakayai, T.; Saebea, D. Energy and exergy analyses of dimethyl ether production using CO and CO₂ hydrogenation. *Int. J. Smart Grid Clean Energy* **2019**, *8*, 544–549. [CrossRef]
49. Farooqui, A.; Di Tomaso, F.; Bose, A.; Ferrero, D.; Llorca, J.; Santarelli, M. Techno-economic and exergy analysis of polygeneration plant for power and DME production with the integration of chemical looping CO₂/H₂O splitting. *Energy Convers. Manag.* **2019**, *186*, 200–219. [CrossRef]
50. Fout, T.; Zoelle, A.; Keairns, D.; Turner, M.; Woods, M.; Kuehn, N.; Shah, V.; Chou, V.; Pinkerton, L. *Cost and Performance Baseline for Fossil Energy Plants Volume 1a: Bituminous Coal (PC) and Natural Gas to Electricity Revision 3*; National Energy Technology Laboratory (NETL): Pittsburgh, PA, USA; Morgantown, WV, USA, 2015; Volume 1a.
51. De Falco, M.; Capocelli, M.; Giannattasio, A. Membrane Reactor for one-step DME synthesis process: Industrial plant simulation and optimization. *J. CO₂ Util.* **2017**, *22*, 33–43. [CrossRef]
52. Dincer, I.; Rosen, M.A.; Khalid, F. Ocean (Marine) Energy Production. In *Comprehensive Energy Systems*; Elsevier: Amsterdam, The Netherlands, 2018; Volumes 3–5.
53. Perry, R.H.; Green, D.W. *Perry’s Chemical Engineers’ Handbook*, 8th ed.; McGraw-Hill: New York, NY, USA, 2013; Volume 53.
54. Demirel, Y.; Sieniutycz, S. Nonequilibrium Thermodynamics: Transport and Rate Processes in Physical and Biological Systems. *Appl. Mech. Rev.* **2003**, *56*, 275–540. [CrossRef]
55. Ertesvåg, I.S.; Kvamsdal, H.M.; Bolland, O. Exergy analysis of a gas-turbine combined-cycle power plant with precombustion CO₂ capture. *Energy* **2005**, *30*, 5–39. [CrossRef]